ORIGINAL ARTICLE

Journal of Cachexia, Sarcopenia and Muscle 2022; **13**: 1197–1209
Published online 30 January 2022 in Wiley Online Library (wileyonlinelibrary.com) **DOI:** 10.1002/jcsm.12919

Cathepsin K activity controls cachexia-induced muscle atrophy via the modulation of IRS1 ubiquitination

Xiangkun Meng[1], Zhe Huang[2,3], Aiko Inoue[4], Hailong Wang[1], Ying Wan[1], Xueling Yue[1], Shengnan Xu[1], Xueying Jin[1], Guo-Ping Shi[5], Masafumi Kuzuya[1,4]* & Xian Wu Cheng[2,3]*

[1]*Department of Community Healthcare & Geriatrics, Nagoya University Graduate School of Medicine, Nagoya, Japan;* [2]*Department of Cardiology and Hypertension, Yanbian University Hospital, Yanji, China;* [3]*Department of Human Cord Stem Cell Therapy, Graduate School of Medicine, Nagoya University, Nagoya, Japan;* [4]*Institute of Innovation for Future Society, Nagoya University Graduate School of Medicine, Nagoya, Japan;* [5]*Department of Medicine, Brigham and Women's Hospital and Harvard Medical School, Boston, MA, USA*

Abstract

Background Cachexia is a complicated metabolic disorder that is characterize by progressive atrophy of skeletal muscle. Cathepsin K (CTSK) is a widely expressed cysteine protease that has garnered attention because of its enzymatic and non-enzymatic functions in signalling in various pathological conditions. Here, we examined whether CTSK participates in cancer-induced skeletal muscle loss and dysfunction, focusing on protein metabolic imbalance.

Methods Male 9-week-old wild-type ($CTSK^{+/+}$, $n = 10$) and CTSK-knockout ($CTSK^{-/-}$, $n = 10$) mice were injected subcutaneously with Lewis lung carcinoma cells (LLC; 5×10^5) or saline, respectively. The mice were then subjected to muscle mass and muscle function measurements. HE staining, immunostaining, quantitative polymerase chain reaction, enzyme-linked immunosorbent assay, and western blotting were used to explore the CTSK expression and IRS1/Akt pathway in the gastrocnemius muscle at various time points. *In vitro* measurements included CTSK expression, IRS1/Akt pathway-related target molecule expressions, and the diameter of C2C12 myotubes with or without LLC-conditioned medium (LCM). An IRS1 ubiquitin assay, and truncation, co-immunoprecipitation, and co-localization experiments were also performed.

Results $CTSK^{+/+}$ cachectic animals exhibited loss of skeletal muscle mass (muscle weight loss of 15%, $n = 10$, $P < 0.01$), muscle dysfunction (grip strength loss > 15%, $n = 10$, $P < 0.01$), and fibre area (average area reduction > 30%, $n = 5$, $P < 0.01$). Compared with that of non-cachectic $CTSK^{+/+}$ mice, the skeletal muscle of cachectic $CTSK^{+/+}$ mice exhibited greater degradation of insulin receptor substrate 1 (IRS1, $P < 0.01$). In this setting, cachectic muscles exhibited decreases in the phosphorylation levels of protein kinase B (Akt^{308}, $P < 0.01$; Akt^{473}, $P < 0.05$) and anabolic-related proteins (the mammalian target of rapamycin, $P < 0.01$) and increased levels of catabolism-related proteins (muscle RING-finger protein-1, $P < 0.01$; MAFbx1, $P < 0.01$) in $CTSK^{+/+}$ mice ($n = 3$). Although there was no difference in LLC tumour growth ($n = 10$, $P = 0.44$), CTSK deletion mitigated the IRS1 degradation, loss of the skeletal muscle mass ($n = 10$, $P < 0.01$), and dysfunction ($n = 10$, $P < 0.01$). *In vitro*, CTSK silencing prevented the IRS1 ubiquitination and loss of the myotube myosin heavy chain content ($P < 0.01$) induced by LCM, and these changes were accelerated by CTSK overexpression even without LCM. Immunoprecipitation showed that CTSK selectively acted on IRS1 in the region of amino acids 268 to 574. The results of co-transfection of IRS1-N-FLAG or IRS1-C-FLAG with CTSK suggested that CTSK selectively cleaves IRS1 and causes ubiquitination-related degradation of IRS1.

Conclusions These results demonstrate that CTSK plays a novel role in IRS1 ubiquitination in LLC-induced muscle wasting, and suggest that CTSK could be an effective therapeutic target for cancer-related cachexia.

Keywords Cachexia; Cathepsin K; Insulin receptor substrate 1; Ubiquitination; Muscle wasting

Received: 28 May 2021; Revised: 22 November 2021; Accepted: 14 December 2021

*Correspondence to: Dr Xian Wu Cheng, Department of Cardiology and Hypertension, Yanbian University Hospital, Yanji 133000, China. Email: chengxw0908@163.com
Dr Masafumi Kuzuya, Department of Community Healthcare & Geriatrics, Nagoya University Graduate School of Medicine, Nagoya 466-8550, Japan. Email: kuzuya@med.nagoya-u.ac.jp
Institution where the study was conducted: Nagoya University, Nagoya, Japan.

Introduction

Cancer cachexia has been defined as an ongoing loss of skeletal muscle mass and function (with or without an accompanying loss of fat mass) that cannot be fully reversed by nutritional therapies.[1,2] Cachexia affects approximately 80% of patients with lung or upper gastrointestinal cancer.[3,4] Cancer cachexia contributes to poor prognosis and severely interferes with patient tolerance to chemotherapy, reducing both quality of life and survival.[5,6] Although cachexia is the primary cause of death in 30% of patients with cancer, it has been estimated that total cancer deaths are underreported by 20–40% and poorly understood to cue cachexia.[2,6] Prevention remains an important goal of cachexia research, and recent studies have called for a focus on therapies to prevent cachexia.[7,8] Cancer cachexia is accompanied by an elevation in inflammatory cytokines, such as tumour necrosis factor-alpha (TNF-α) and interleukin-6 (IL-6), which induce alterations in the metabolism of proteins, carbohydrates, and lipids.[9,10] Among these changes, muscle fibre protein metabolism is especially significant due to its role in maintaining muscle function and mass.[11] Cancer cachexia suppresses the mammalian target of rapamycin (mTOR) phosphorylation and activates muscle atrophy F-box gene (MAFbx1), both of which are major protein metabolism targets located downstream of the insulin-like growth factor 1 (IGF1)/insulin receptor substrate 1 (IRS1) signalling pathway.[12,13] Recent studies have shown that cancer cachexia induces IGF1/IRS1 pathway suppression.[14,15] Reactivation of the IGF1/IRS1 pathway might also have potential as a therapeutic strategy to prevent cancer-cachexia-induced muscle atrophy by improving the protein metabolism imbalance.

Cathepsin family expression is up-regulated during various forms of skeletal muscle atrophy.[16,17] Numerous studies over the previous decade have identified CTSK expression in many common human cancers.[18,19] In addition to its function as an endopeptidase, CTSK directly degrades proteins via the actions of a covalently cross-linked substrate.[20] Recent evidence suggests that CTSK plays a significant role in the reducing myofibril proteins such as desmin in a skeletal and myocardial muscle injury model.[16,21] CTSK deficiency improved the weight loss and cardiac contractile dysfunction in diabetic mice.[22,23] CTSK deficiency partially restores alterations in insulin resistance.[22,24] In several mouse models, CTSK deletion improved the pathologically dampened phosphorylation of protein kinase B (Akt) located downstream of the IGF1/IRS1 signalling pathway, which promotes protein anabolism and prevents cardiac mass loss and dysfunction.[21,22]

In this study, we explored the role(s) of CTSK in the pathogenesis of cachexia-related muscle atrophy in mice under tumour-bearing conditions. Cachexia-related muscle mass loss and dysfunction were studied in CTSK-knockout ($CTSK^{-/-}$) and wild-type ($CTSK^{+/+}$) mice that were injected with murine Lewis lung carcinoma cells (LLC). In a separate *in vitro* experiment, we used C2C12 mouse myoblasts to investigate the role of CTSK on IRS1 and the signalling pathway downstream of IRS1. We found that the silencing of CTSK increased IRS1 levels and the signalling pathway downstream of IRS1 in C2C12 cells treated with LLC-conditioned medium (LCM). The IRS1 levels and the signalling pathway downstream of IRS1 were decreased by the overexpression of CTSK in C2C12 cells without LCM conditions. Under our experimental conditions, these results might provide the first evidence and mechanistic explanation of the CTSK-mediated regulation of IGF1/IRS1 signalling in muscle atrophy. We propose that CTSK is an essential molecular determinant of muscle atrophy in cancer patients and a potential therapeutic target.

Materials and methods

Materials and methods used in this study are described in the supporting information.

Statistical analysis

Data are expressed as means ± standard error of the mean. Following the test of the data distribution status by Shapiro–Wilk's test, the data were subjected to statistical analysis using Student's *t*-test for comparisons between two groups or one-way analysis of variance for comparisons of three or more groups; both tests were followed by Tukey's post hoc test. A two-way repeated-measurement analysis of variance and Bonferroni post hoc test were subjected to the data of body weight, grip strength, and so on. Statistical significance was set at $P < 0.05$.

Results

Cancer induces skeletal muscle mass loss, dysfunction, and inflammation

A mouse LLC model has often been used to investigate cachexia-related muscle disorders. To test our hypothesis that cachexia affects CTSK expression, we used a mouse model of cachexia induction by LLC injection to examine CTSK

mRNA and protein expression in the skeletal muscles of CTSK$^{+/+}$ mice. The CTSK$^{+/+}$ tumour-bearing (WL) mice exhibited the cachexia phenotype. As shown in *Figure* 1A, there was a significant reduction in the rate of body weight change from 21 to 28 days after LLC injection. Cachexia resulted in a decrease in the gastrocnemius (GAS) and soleus weights of WL mice from Days 14 or 28 after LLCs injection (*Figures* 1B and S6B). As anticipated, WL mice showed a marked reduction in the grip strength (*Figure* 1C). ELISA data revealed that serum TNF-α protein levels were markedly increased in the WL mice from Days 21 to 28 compared with the Day 0 (*Figure* 1D). Macrophages were found in the implanted tumours stripped from mice (*Figure* 1E). On Day 28, quantitative H&E staining showed a significant reduction in the myofibre cross-section area in the GAS muscles of WL mice compared with those of CTSK$^{+/+}$ control (WC) mice (*Figure* 1F and 1G). *Figure* S1A shows the time-dependent changes in the tumour weights of WL mice. To identify potential mechanisms of cachexia development in the LLC mouse model, we analysed three isoforms of cathepsins (S, K, and L) in the control and cachectic GAS of CTSK$^{+/+}$ mice. qPCR revealed that only the expression of CTSK increased linearly with tumour growth, while the expressions of the other cathepsin isoforms were markedly up-regulated at the last day of cachexia induction (*Figures* 1J, S1B and S1C). *Figures* 1K, S1D, S1E, and S6F show that the CTSK protein was highly expressed and activated in the cachectic GAS muscle in a time-dependent manner. The immunohistochemical analysis confirmed these changes in CTSK. LLC tumours can increase the number and percentage of muscle fibres with high CTSK expression (*Figure* 1F, 1H, and 1I). CTSK is highly expressed in type I fibres in the WC group. Under cachexia conditions, tumours may increase the content of CTSK in type I and II muscle fibres to cause muscle atrophy (*Figure* S7B). Western blotting results showed that the protein catabolism-related muscle-specific ring finger protein 1 (MuRF1), an essential marker for muscle atrophy, was activated in cachectic GAS muscles (*Figure* S1D and S1F). The WL group, not the CTSK$^{-/-}$ tumour-bearing (KL) group, showed increased CTSK levels in serum on the 28th day (*Figures* 1L and S6G). Combined with *Figure* 1K and 1L that CTSK content increased in GAS muscle (Day 21) earlier than in serum, CTSK is derived from muscle rather than the tumour. These observations indicate that CTSK-mediated protein catabolism might have contributed to the muscle mass

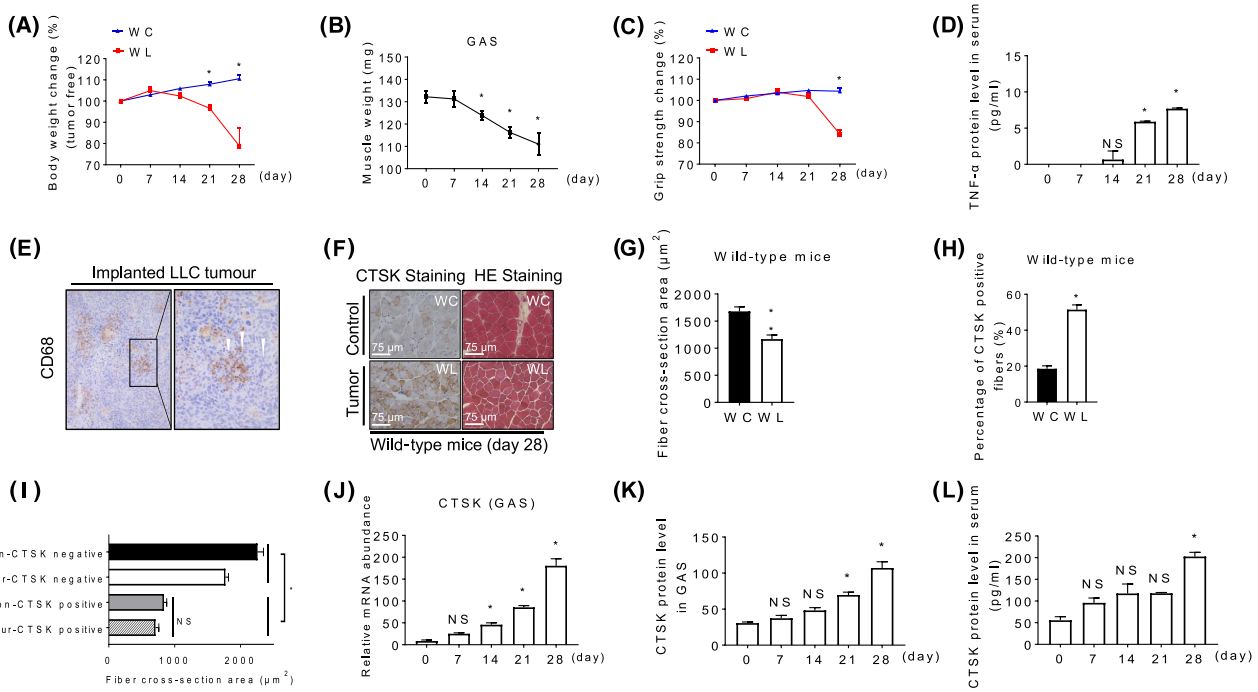

Figure 1 Cancer-induced skeletal muscle mass loss, dysfunction, and inflammation. (*A*) The bodyweights of tumour-bearing (WL) and non-tumour-bearing control (WC) mice. (*B*) GAS muscle weight measurements of WL mice at the indicated time points (n = 5 for each time point). (*C*) Grip strength analysis of WL and WC mice. (*D*) ELISA analysis of TNF-α in serum from WL mice at the indicated time points (n = 5 for each time point). (*E*) Immunohistochemistry with CD68 antibody for the infiltrated macrophages in the implanted tumour cross-sections of WL mice. (*F–I*) Representative images of CTSK and H&E staining (*F*) and combined quantitative data for the fibre cross-section area (*G*), the percentage of CTSK-positive fibre (*H*), and the area of CTSK-positive fibres at day 28 after LLC or vehicle injection (*I*). (*J*) qPCR analysis of CTSK in GAS muscles (n = 5). (*K* and *L*) ELISA analysis of CTSK in GAS muscles and serum from tumour-bearing mice at the indicated time points (n = 5 for each time point). Data are the means ± SEM, and P values were determined by two-way repeated measures ANOVA and Bonferroni's post hoc tests (*A*,*C*), one-way ANOVA followed by Tukey's post hoc tests (*B*,*D*,*I*,*J*,*K*, and *L*), or unpaired Student's t-test (*G*,*H*). WC, CTSK$^{+/+}$ control; WL, CTSK$^{+/+}$ tumour-bearing.

DOI: 10.1002/jcsm.12919

loss of mice under our experimental conditions. There were no differences in the apoptosis of the GAS muscles between the WL and WC mice as determined by ssDNA-staining assay (*Figure* S2A).

CTSK deletion prevents muscle wasting and dysfunction without affecting tumour growth and TNF-α levels in LLC tumour-bearing mice

To determine whether CTSK is required for the development of cancer-induced cachexia, we implanted the LLC cells into the subcutaneous of KL and WL mice. As shown in *Figure* 2A, CTSK deficiency resulted in significantly higher bodyweight compared with that in WL mice. The weights of GAS and soleus muscles of the WL mice were lower than the corresponding weights in the WC mice. In contrast, KL mice exhibited almost no loss of muscle mass compared with CTSK$^{-/-}$ control (KC) mice (*Figures* 2B and S6C). The grip strength monitoring revealed that the grip strength of the WL mice declined in parallel with the muscle weights; these changes were markedly rectified by CTSK deletion at the latter two time points (*Figure* 2C), suggesting that CTSK deficiency can preserve cachectic muscle mass and function. As anticipated, quantitative data of H&E staining analysis revealed that the GAS muscle fibre cross-section area was higher in the KL mice than the WL mice (*Figure* 2D and 2E). As shown in *Figures* 2F–2H and S6A, we observed no significant differences in tumour growth, food intake or serum IL-6 and TNF-α protein levels between WL and KL mice. Together, these observations suggest that CTSK$^{-/-}$-mediated muscle protection is not attributable to the influence of CTSK deficiency on tumour growth and systemic inflammation. We also observed no differences in the body and muscle weights, serum TNF-α and IL-6 levels, or muscle fibre cross-section areas between WC and KC mice at baseline (*Figure* 2A–2C, 2E, 2G, and 2H).

To determine whether CTSK affects muscle protein metabolism in cachexia, we investigated pathways associated with the anabolic and catabolic effects of muscle proteins in WL and KL mice. *Figures* 3A, 3B, S6D, and S6E showed that the intracellular IRS1 levels were decreased in the muscle isolated from WL mice. In CTSK$^{-/-}$ mice, as in KC mice, even though the tumour-bearing CTSK$^{-/-}$ muscles still contained an abundant amount of IRS1 protein (*Figure* 3A and 3B), the levels of insulin-like growth factor 1 receptor (IGF1R), the upstream protein of IRS1, did not change significantly in any of the four groups (*Figure* 3A). Notably, the PCR results also showed no differences in the IRS1 gene expression among the four experimental groups (*Figure* 3C), indicating that CTSK regulates the IRS1 level mainly at the posttranscriptional level. IRS1, which is known as the insulin/IGF-1 signalling pathway components, is significantly reduced in the cachexia microenvironment, which may cause muscle atrophy, hypoglycaemia, glucose insensitivity, and other diabetes-like symptoms. Our experiments show that increased CTSK might modulate skeletal muscle protein catabolism and anabolic metabolism by degrading IRS1 in cachectic mice. This notion was supported by the results of western blotting and quantitative PCR, which showed that the WL muscles exhibited harmful change

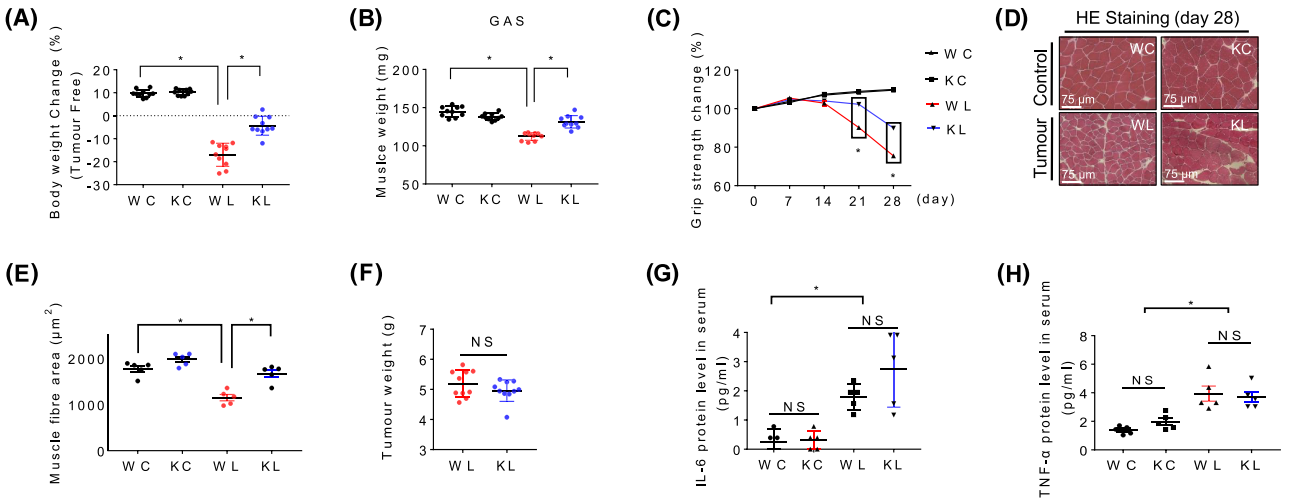

Figure 2 CTSK deletion prevented muscle wasting and dysfunction without affecting tumour growth or TNF-α in tumour-bearing mice. (*A*) The bodyweight and (*B*) GAS muscle weight analysis of the four groups of mice (WC, KC, WL, and KL; *n* = 10) on the 28th day after tumour implantation. (*C*) The measurements of forelimb grip strength in the four groups of mice at the indicated time points (*n* = 10 for each group). Representative HE images (*D*) and quantitative data (*E*) for the cross-sections of GAS muscles harvested from the four groups of mice on Day 28. (F) Tumour weight measurements derived from the WL and WC mice (*n* = 10). (*G*, *H*) ELISA analyses of serum IL-6 and TNF-α protein levels in the four experimental groups at Day 28 after tumour implantation (*n* = 5 for each group). Data are means ± SEM, and *P* values were determined by two-way repeated measures ANOVA and Bonferroni's post hoc tests (*C*), one-way ANOVA followed by Tukey's post hoc tests (*A*,*B*,*E*,*G*, and *H*), or unpaired Student's *t*-test (*F*). WC, CTSK$^{+/+}$ control; KC, CTSK$^{-/-}$ control; WL, CTSK$^{+/+}$ tumour-bearing; KL, CTSK$^{-/-}$ tumour-bearing.

DOI: 10.1002/jcsm.12919

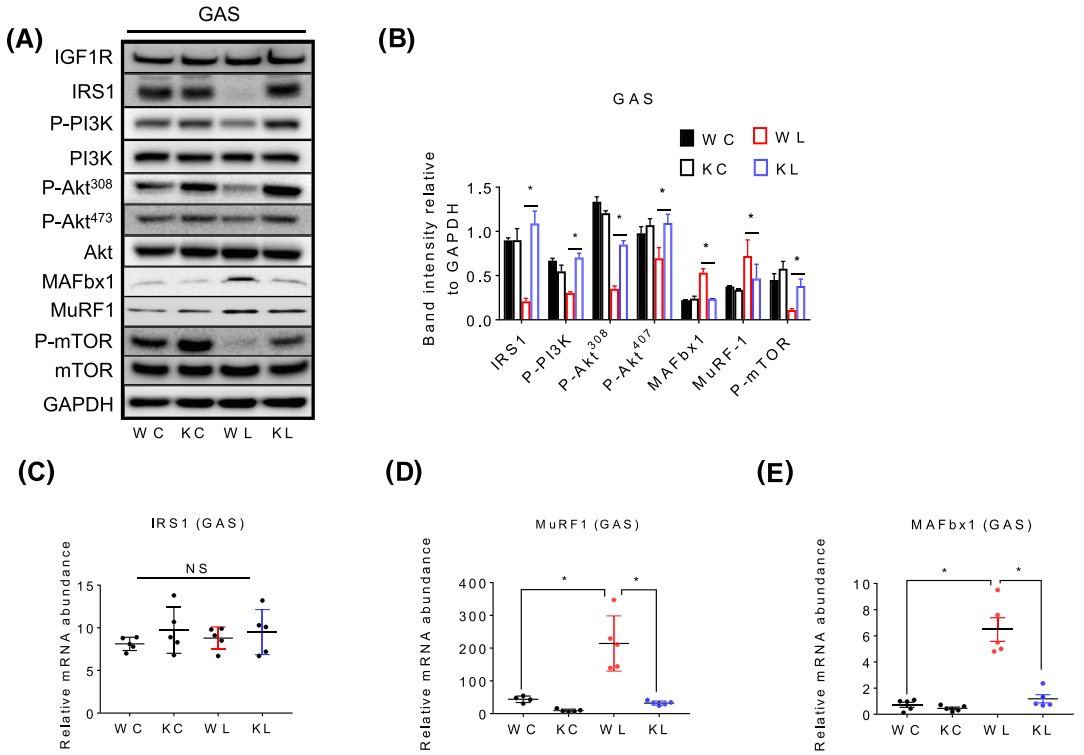

Figure 3 CTSK deletion ameliorated anabolic and catabolic molecular alterations in the cachectic muscles. (*A*,*B*) Representative immunoblotting images and quantitative data for IGF1R, IRS1, P-PI3K, P-Akt^{308}, P-Akt^{473}, MAFbx1, MuRF1, and P-mTOR in GAS muscles at Day 28 after tumour implantation (n = 3). (*C*–*E*) qPCR analysis of IRS1, MuRF1, and MAFbx1 in GAS muscles (n = 5). GAPDH serves as an internal loading control. Data are means ± SEM, and P values were determined by one-way ANOVA followed by Tukey's post hoc tests (*B*–*E*). WC, CTSK$^{+/+}$ control; KC, CTSK$^{-/-}$ control; WL, CTSK$^{+/+}$ tumour-bearing; KL, CTSK$^{-/-}$ tumour-bearing.

in the levels of MuRF1, MAFbx1, phosphoinositide 3-kinase (P-PI3K), P-Akt^{308}, P-Akt^{473}, and P-mTOR proteins and/or genes (*Figures* 3A, 3B, 3D, 3E, S6D, and S6E).

CTSK up-regulation and IRS1 degradation in LCM/TNF-α-treated cells

To test the effect of tumour-released factors on CTSK expression, we analysed the C2C12 myotubes treated with 0%, 25%, and 50% LCM (Con, LCM1/4, and LCM1/2, respectively). As shown in *Figure* 4A, CTSK mRNA expression was sensitive to the stimulators LCM1/2. Consistently, LCM resulted in increased CTSK protein expression and activities in a dose-dependent manner (*Figures* 4B, S2B, and S7C), indicating that the up-regulation of CTSK expression is associated explicitly with tumour-released factors in C2C12 cells. We found that macrophages infiltrated the tumour tissues under our present experimental conditions. TNF-α elevation has been reported in the serum of mouse cachexia models and patients with advanced cancers.[25] We observed that TNF-α stimulates CTSK expression and activities in a time-dependent manner (*Figures* 4A, 4C, S2C, and S7C). To clarify the effect of TNF-α on the promoter of CTSK, we conducted a reporter assay. The results showed that the expression of NlucP was significantly increased after stimulation with TNF-α (100 ng/mL) for 24 h (*Figure* 4D). This result indicates that TNF-α can promote CTSK expression by activating the CTSK promoter. Together with the finding that the serum TNF-α levels were increased in a time-dependent manner in WL mice (*Figure* 1D), these results indicated that TNF-α secreted from tumour-associated inflammatory cells may contribute to the process of muscle atrophy via the regulation of CTSK expression. The representative western blotting images showed that LCM decreased the levels of the P-IRS1, IRS1, P-Akt^{308}, and P-Akt^{473} proteins and increased the levels of Forkhead box O3 (FOXO3) protein in a dose-dependent manner but had no effect on IGF1R (*Figures* 4B and S2B). *Figures* 4E and S2F show that LCM-induced myotube atrophy. Recombinant human TNF-α decreased the IRS1 protein content in a time-dependent manner but had no effect on IGF1R (*Figures* 4C and S2D). The expressions of the FOXO1, FOXO3, and MAFbx1 genes were all sensitive to LCM1/2 stimulation, and the MAFbx1 and MuRF1 genes were sensitive to TNF-α stimulation (*Figures* 4F, 4G, S2E, 7D, and 7E), suggesting that LCM and TNF-α could induce the protein metabolism imbalance in the myotubes. Notably, TNF-α and LCM reduced the content of IRS1 but did not affect the mRNA level (*Figure* 4H), suggesting that the decrease in IRS1 content was due to the degradation of IRS1 rather than a change in

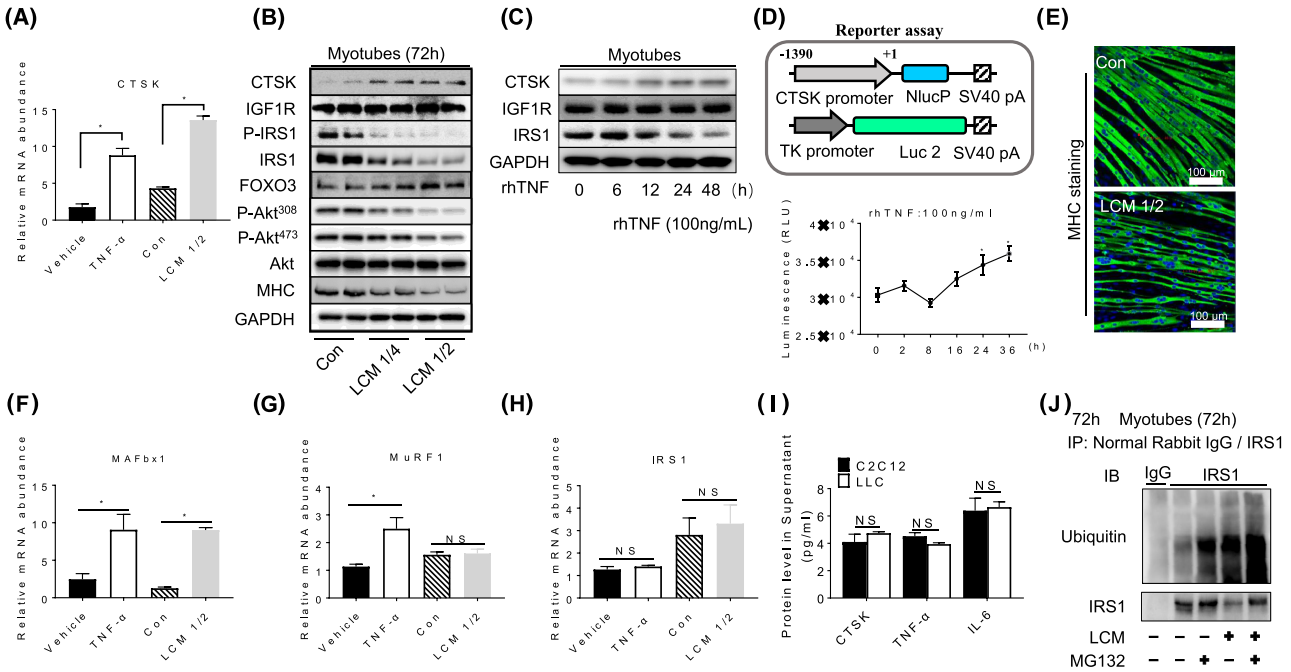

Figure 4 CTSK was up-regulated, and IRS1 was degraded in C2C12 myotubes and myoblasts in response to TNF-α or LCM1/2. (*A*) C2C12 cells were grown in differentiation medium for 5 days to differentiate the myoblasts, treated with/without TNF-α (100 ng/mL) for 48 h, or treated with/without LCM1/2 medium for 72 h, and then, the cells were applied to detect the expression levels of CTSK mRNA by qPCR. (*B*) The differentiated myoblasts were treated with or without LCM1/4 or LCM1/2 medium for 72 h, and then, the cell lysates were subjected to Western blotting using the indicated antibodies. (*C*) The differentiated myoblasts were treated with TNF-α (100 ng/mL) at the indicated time points and then were subjected to western blotting using the indicated antibodies. (*D*) Schematic representation depicting the reporter assay vector (upper panel). The C2C12 cells were co-transfected with CTSK-promoter-Nluc vector and pTK-promoter-Luc2 vector for 24 h. Then, the cells were treated with 100 ng/mL of TNF-α for the indicated time points and subjected to luminescence measurement using a Nano-Glo Dual-Luciferase Reporter Assay System (lower panel). (*E*) Following differentiation for 7 days, the differentiated myoblasts were treated with control DMEM or LCM1/2 for 72 h and then were subjected to immunofluorescence staining of MHC. (*F–H*) The mRNA expression levels of MAFbx1, MuRF1, and IRS1 in differentiated C2C12 cells treated with LCM and TNF-α. (*I*) An ELISA assay was performed to determine the levels of CTSK, TNF-α, and IL-6 in the LLC and C2C12 supernatant. (*J*) Following differentiation for 5 days, the differentiated myoblasts were replaced with LCM1/2-conditioned medium in the presence of G5 with/without MG132 for 72 h. Immunoprecipitation was then performed with non-immune rabbit IgG or an antibody for endogenous IRS-1. Data are means ± SEM, and *P* values were determined by unpaired Student's *t*-test (*I*), or one-way ANOVA followed by Tukey's post hoc tests (*A*,*D*,*F*,*G*, and *H*).

the transcription level of mRNA. In the cell supernatant analysis, the ELISA data showed that there were no differences in the levels of the CTSK, TNF, or IL-6 proteins between the supernatant of C2C12 cells and LLC (*Figure* 4I). This result further confirmed that the LCM-induced CTSK high expression was derived from intracellular C2C12 and not from the exosome of LLC.

To identify the mechanism of LCM promotes IRS1 degradation, we performed immunoprecipitation using C2C12 myotubes treated with LCM1/2 in the presence or absence of the proteasome inhibitor MG132. LCM decreased the content of IRS1 protein in the lysates, and this effect was rectified by MG132 (*Figure* 4J), indicating that LCM can down-regulate IRS1 content by promoting its ubiquitination and subsequent proteasome-mediated degradation.

CTSK directly cleaves IRS1

To elucidate the specific role of CTSK in the degradation of IRS1, we used an HEK cellular transfection system combined with a proteasome inhibitor. HEK cells were co-transfected with HA or CTSK-HA with four different lengths of IRS1-FLAG (C-terminal; 1–1243, 1–865, 1–574, and 1–268) for 72 h, and then the cells were treated with MG132 for 5 h. The results of immunoprecipitation showed that CTSK selectively acted on IRS1 within the region of amino acids 268 to 574, leading to an increase in its ubiquitination level (*Figure* 5A). To further confirm that CTSK acted directly on IRS1, the C2C12 cells were co-transfected with IRS1-mCherry and CTSK-EGFP for 24 h. Immunofluorescence staining showed abundant intracellular co-localization of CTSK and IRS1 in C2C12 cells (*Figure* 5B). We investigated the role of CTSK and CTSK^{mut} (Y67L and L205A mutants)[26] in IRS1 truncations. The results showed that CTSK, but not CTSK^{mut}, promoted the loss of IRS1 content compared with the vehicle (*Figure* 5D), indicating that CTSK might interact directly with the PTH domain of IRS1 (*Figure* 5D). Several studies have reported that cathepsin family members such as CTSS and CTSD cleaved the domain of target proteins and thereby decreased their stability and

DOI: 10.1002/jcsm.12919

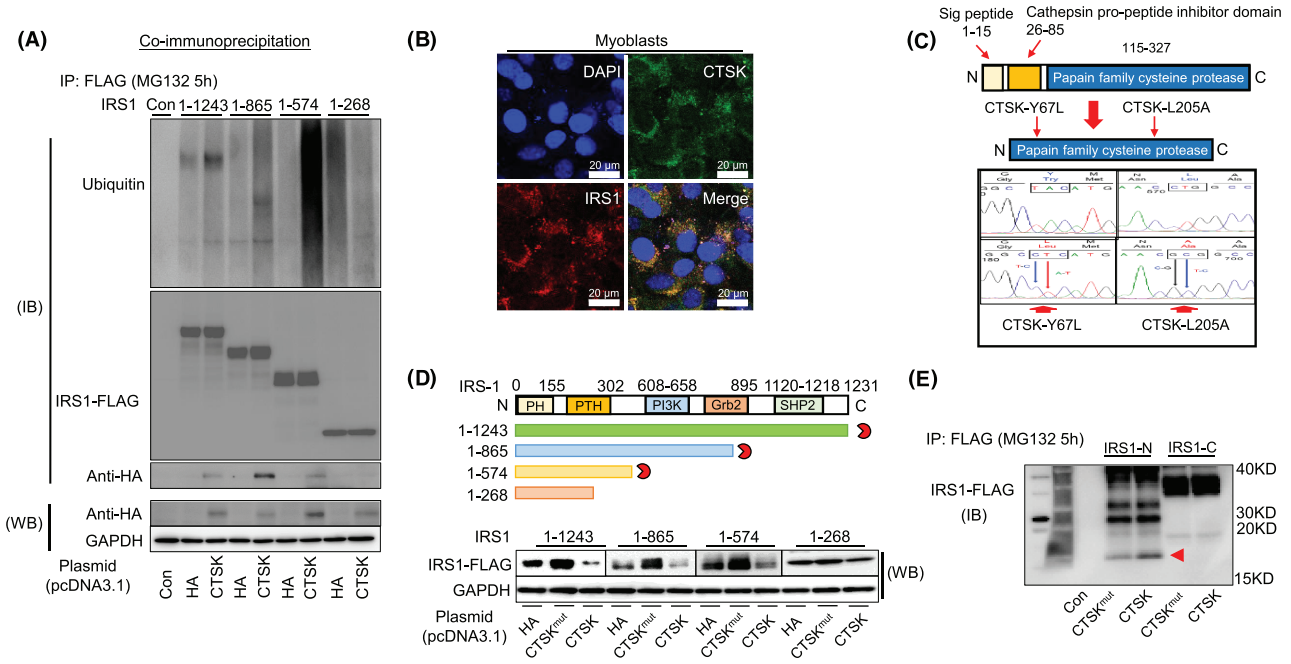

Figure 5 CTSK directly cleaved IRS1. (*A*) C2C12 cells were co-transfected with different lengths of IRS-1-3xFLAG (1–1243, 1–865, 1–574, 1–268) for 72 h, and then, the cells were treated with MG132 for 5 h. The cell lysates (1 mg) were immunoprecipitated with FLAG M2 magnetic beads. The eluate was analysed by western blotting. (*B*) C2C12 cells were co-transfected with pcDNA3.1-IRS1-mCherry and pcDNA3.1-CTSK-EGFP for 24 h. The cells were subjected to immunofluorescence staining and observed under a confocal microscope. (*C*) Schematic representation depicting the CTSK protein domain and sequence results for mutation of the CTSK construct. (*D*) Schematic representation of IRS-1 deletion mutants fused with C-terminal 3xFLAG. The C2C12 cells were co-transfected with vectors expressing the wild-type CTSK-HA or mutant CTSK (Y67L/L205A)-HA and different lengths of IRS-1-3xFLAG. After 72 h, the cell lysates were subjected to western blotting. (*E*) HEK293 cells were co-transfected with C-terminal 3xFLAG- or N-terminal 3xFLAG-tagged IRS1 plasmids and wild-type CTSK-HA or mutant CTSK(Y67L/L205A)-HA, respectively. After 72 h, cells were treated with MG132 for 5 h, followed by immunoprecipitation with FLAG M2 magnetic beads. The eluate was analysed by western blotting.

led to their degradation by the proteasome.[27,28] We generated IRS1-C-terminal-FLAG (IRS1-C) and IRS1-N-terminal-FLAG (IRS1-N). Following co-transfection of IRS1-N or IRS1-C with CTSK, respectively, the lysates were reacted with FLAG antibody. *Figure* 5E shows that a new bond (red arrow) appeared. Taken together, these findings suggest that CTSK selectively cleaves IRS1 and causes ubiquitination-related degradation of IRS1.

CTSK decreases the content of IRS1 in C2C12 cells

To determine whether CTSK regulated IRS1 degradation, we also checked the IRS1 stability in C2C12 cells after CTSK overexpression. A protein synthesis inhibitor named cycloheximide, which discriminates between the degradation of IRS1 and its synthesis, was used to determine the degradation rate of IRS1. C2C12 myoblasts were co-transfected with IRS1-FLAG and HA or CTSK, respectively, for 48 h. Then the cells were treated with cycloheximide for the indicated amounts of time. In C2C12 myoblasts, IRS1 was degraded upon CTSK expression in a time-dependent manner (*Figure* 6A). To test whether CTSK mediated the IRS1 loss in myotubes, we monitored IRS1 content in lentivirus-mediated CTSK-overexpressed C2C12 myotubes. As shown in *Figure* 6B and 6C, IRS1 content was dramatically decreased by CTSK overexpression. This effect still existed in the presence of LCM, and the increased expression of CTSK enhanced the degradation of IRS1 (*Figure* S5C and S5D). In lentivirus-mediated CTSK-silenced C2C12 myotubes, under an LCM1/2 condition, IRS1 protein was markedly accumulated compared with the control (*Figure* 6D and 6E). This effect also exists when LCM does not exist (*Figure* S5A and S5B). The results in *Figure* 6F–6H show that CTSK overexpression induces myotube atrophy and CTSK silence improves the LCM-induced myotube atrophy. These data indicate that CTSK negatively regulates IRS1 content. Lentivirus-CTSK as well as pcDNA3.1-CTSK increased CTSK protein expression and shRNA-CTSK inhibited CTSK protein expression (*Figure* 6B–6E).

CTSK promotes IRS1 degradation by ubiquitination

Because it has been reported that IRS1 stability is regulated by ubiquitin proteolysis,[29] we examined the effect of CTSK on the ubiquitination of IRS1. The immunoprecipitation results showed that the IRS1 ubiquitination level was increased in the presence of CTSK overexpression (*Figure* 7A). CTSK overexpression accelerated IRS1 loss in C2C12 cells. The decrease in IRS1 content was not observed in the Y67L and L205A mutants[26] (*Figure* 7B and 7C), suggesting that the function sites of CTSK are essential for the IRS1 content loss

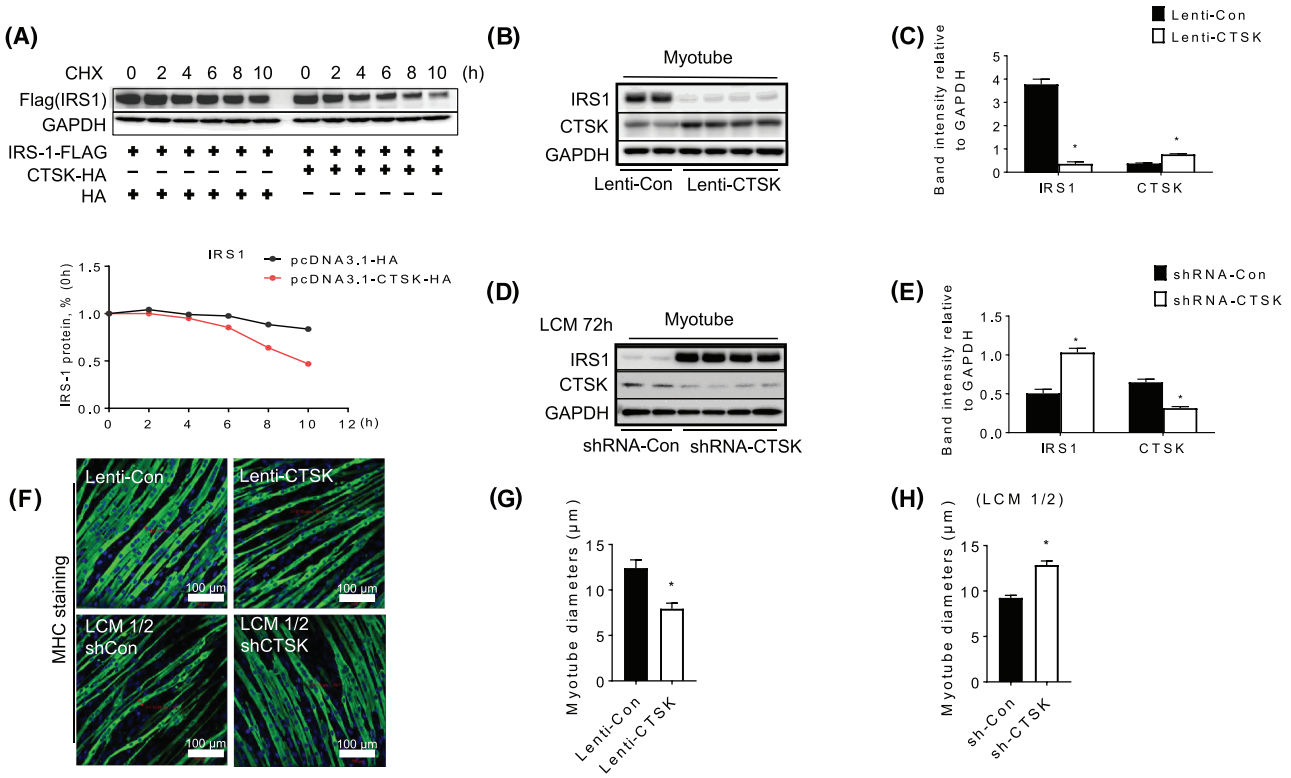

Figure 6 CTSK promoted IRS1 degradation. (*A*) C2C12 cells were co-transfected with pcDNA3.1-CTSK-HA and pcDNA3.1-IRS-1-3xFLAG plasmids for 48 h to express equivalent levels of IRS-1, and then treated with cycloheximide (CHX) for various amounts of time. The lysates were subjected to western blot analysis. (*B*,*C*) C2C12 myoblasts inducible expressing CTSK-HA were grown in differentiation medium for 5 days to differentiate the myoblasts, and then, the cells were treated with DOX for 72 h. Cells were harvested and separated on SDS-PAGE gel followed by immunoblot analysis to detect endogenous IRS-1 levels. (*D*,*E*) Following differentiation for 5 days, the stable-cell line (CTSK-shRNA or control-shRNA) was cultured with 500 ng/mL doxycycline (DOX) and LCM1/2 for 72 h. Cells were harvested and subjected to immunoblot analysis to detect endogenous IRS-1 levels. (*F*) Upper panel: the myotubes with lentivirus-CTSK or -control were induced with 500 ng/mL doxycycline (DOX) for 72 h. Lower panel: in the presence of LCM1/2, the myotubes with CTSK-shRNA or control-shRNA were induced with 500 ng/mL doxycycline (DOX) for 72 h. Then, the myotubes were subjected to immunofluorescence staining of MHC. Quantification of the mean myotube diameter of (*G*) Lenti-Con/Lenti-CTSK- and (*H*) shCon/shCTSK-myotubes. Data are means ± SEM, and *P* values were determined by unpaired Student's *t*-test (*C*,*E*,*G*, and *H*).

(*Figure* 7B and 7C). These observations indicated that CTSK decreases IRS1 content by increasing the IRS1 ubiquitination. To further demonstrate the role of CTSK in IRS1 degradation in muscle cells, we transfected small siRNA-Con or siRNA-CTSK into C2C12 myoblasts under an LCM1/2 condition. The immunoprecipitation results showed that CTSK silencing also decreased the IRS1 ubiquitin level (*Figure* 7D). The CTSK silencing induced an accumulation of IRS1 in LCM1/2-treated C2C12 cells (*Figure* 7E and 7F), suggesting that CTSK silencing prevented the IRS1 from ubiquitination and degradation in C2C12 cells treated with LCM. We examined the effect of CTSK on the ubiquitination of IRS1 in cells treated with LCM 1/2. The immunoprecipitation results showed that the IRS1 ubiquitination level increased in the presence of CTSK overexpression under LCM conditions (*Figure* 7G). CTSK overexpression accelerated IRS1 loss in C2C12 cells treated with LCM (*Figure* 7H and 7I). These observations indicated that CTSK decreases IRS1 content by increasing the IRS1 ubiquitination. The pcDNA3.1-CTSK/pcDNA3.1-CTSK^{mut} increased CTSK protein expression and siRNA-CTSK reduced it (*Figure* 7B, 7E, and 7H).

Genetic modifications of CTSK modulate protein catabolism and myosin heavy chain content via regulation of the IRS/Akt 1-signalling pathway

To determine whether the CTSK-mediated control of IRS1 degradation contributes to the IRS1/Akt-signalling pathway in skeletal muscle, we examined the phosphorylation of Akt^{308}, Akt^{473}, mTOR, and the contents of MHC, MAFbx1 in CTSK-overexpressing C2C12 myotubes and myoblasts. As shown in *Figures* 8A, 8B S3A, and S3B, the phosphorylation of Akt^{308}, Akt^{473}, and mTOR was dramatically decreased by CTSK overexpression in myotubes (for lentivirus-CTSK) and myoblasts (for pDNA3.1-CTSK). Under the LCM1/2 conditions (*Figure* S5C–S5F), phosphorylation of Akt^{308}, Akt^{473}, and mTOR was also dramatically decreased by CTSK overexpression. The IRS1/Akt-signalling pathway was analysed in the lentivirus-mediated CTSK-silenced C2C12 myotubes and

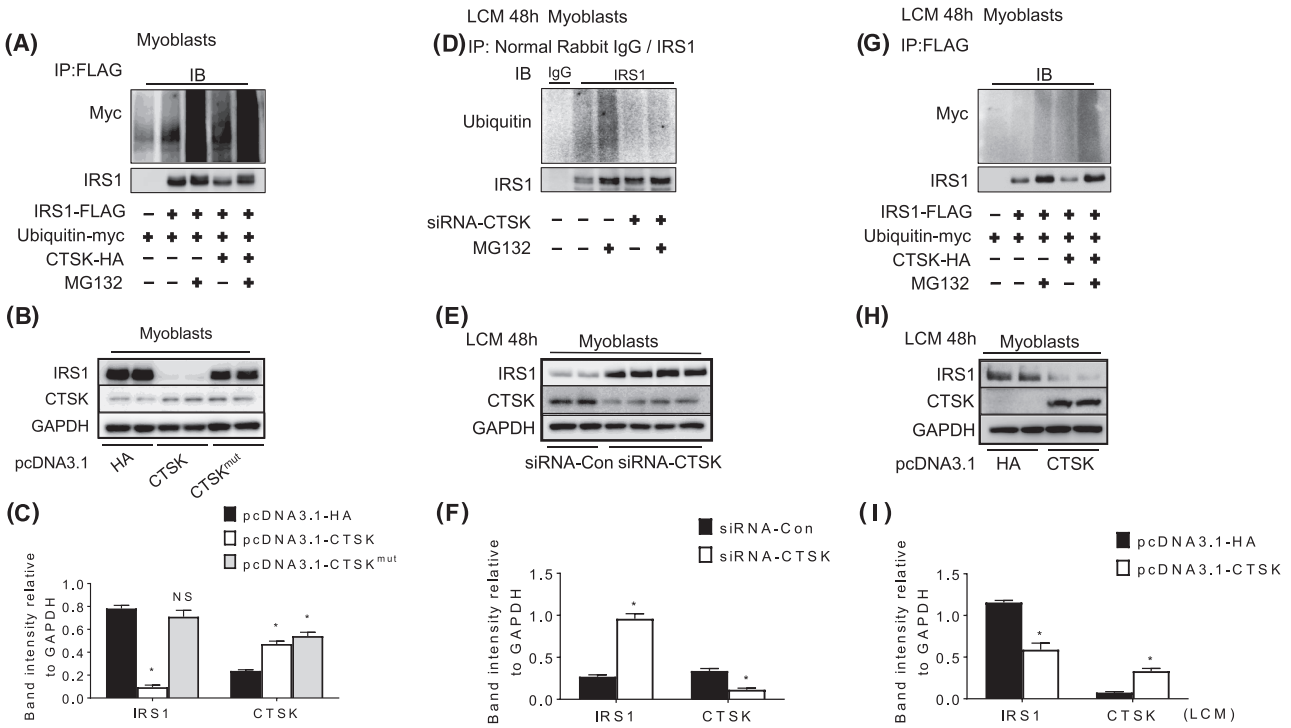

Figure 7 Ubiquitin was involved in CTSK-mediated IRS1 degradation. Cells were harvested and subjected to immunoblot analysis to detect endogenous IRS-1 ubiquitin levels and IRS1 content. (*A*) The ubiquitination analysis: C2C12 cells were co-transfected with pcDNA3.1-IRS-1-3xFLAG, pcDNA3.1-CTSK-HA/pcDNA3.1-HA, and pCMV-Myc-Ub plasmids for 72 h, and then cultured in the presence of G5 with/without MG132 for 5 h. To reveal polyubiquitination, whole-cell lysates (~1 mg of protein) from C2C12 cells were immunoprecipitated with FLAG M2 magnetic beads. The precipitates were separated by SDS-PAGE, followed by immunoblotting with myc-tag antibodies. (*B*) Immunoblot analysis of CTSK, IRS1, and GAPDH in whole-cell lysates of C2C12 cells, which were transfected with pcDNA3.1/pcDNA3.1-CTSK-HA/inactivated pcDNA3.1-CTSK (Y67L, L205A)-HA plasmids and pcDNA3.1-IRS-1-3xFLAG plasmids. (*C*) The quantitative data for IRS1 and CSTK. (*D*) The C2C12 cells were transfected with Con- or CTSK-siRNA, and then, the cells were treated with LCM1/2. After 48 h, cells were treated with G5 with or without MG132 for 5 h. The whole-cell lysates were analysed by immunoblot with anti-ubiquitin and anti-IRS-1 antibody. (*E*,*F*) Representative immunoblot images and quantitative analysis of CTSK, IRS1, and GAPDH in whole-cell lysates of LCM-stimulated CTSK-silenced or control C2C12 cells. (*G*) C2C12 cells were co-transfected with pcDNA3.1-IRS-1-3xFLAG, pcDNA3.1-CTSK-HA/pcDNA3.1-HA, and pCMV-Myc-Ub plasmids and then treated with the LCM1/2 for 48 h. (*H*) Immunoblot analysis of CTSK, IRS1, and GAPDH in whole-cell lysates of LCM-stimulated C2C12 cells, which were transfected with pcDNA3.1-HA or pcDNA3.1-CTSK-HA and pcDNA3.1-IRS-1-3xFLAG plasmids. (*I*) The quantitative data for IRS1 and CSTK. Data are means ± SEM, and *P* values were determined by one-way repeated measures ANOVA and Tukey's post hoc tests (*C*) or unpaired Student's *t*-test (*F* and *I*).

siRNA-CTSK-silenced myoblasts under the LCM1/2 conditions. In both groups, CTSK silencing resulted in an increase in P-Akt and P-mTOR protein levels in response to LCM1/2 (*Figures* 8C, 8D, S3C, and S3D). Without the LCM stimulation (*Figure* S5A and S5B), it is worth noting that, although CTSK silence increased the IRS1 content in myotubes, it had little effect downstream of IRS1. These results indicate that the genetic modifications of CTSK negatively or positively modulated IRS1-signalling pathway activation in C2C12 cells. We also observed that CTSK overexpression induced a decrease in MHC and an increase in MAFbx1, and these changes were diminished by CTSK silencing under LCM conditions (*Figures* 8A–8D and S3A–S3D).

To further confirm the effect of IRS1 on the downstream IRS1-signalling pathway, the C2C12 myoblasts treated with siRNA-IRS1 or IRS1-plasmid, respectively, were analysed by western blotting assay. As anticipated, siRNA-IRS1 decreased the IRS1 protein expression (*Figures* 8E and S4A). IRS1 silencing effectively inhibited the phosphorylation of Akt and mTOR in C2C12 cells (*Figures* 8E and S4A). The phosphorylation levels of Akt and mTOR were not affected by IRS1 overexpression (*Figures* 8F and S4B), suggesting that IRS1 overexpression did not affect downstream signal activation under our experimental conditions. Because IGF1-Akt/mTOR signalling inactivation seemed to be tightly associated with muscle protein loss,[30,31] we used an inhibitor of IRS1 (NT157) and an inhibitor of Akt (X) to extend our examination to the interaction of IRS1 with Akt. The results showed that IRS1 and Akt inhibitions induced a harmful change in the levels of IGF1-induced P-Akt and/or P-mTOR and MAFbx1 proteins in C2C12 myotubes (*Figures* 8G, 8H, S4C, and S4D). The Akt inhibitor reduced the content of MHC, which was an important structural protein for skeletal muscle (*Figures* 8H and S4D).

DOI: 10.1002/jcsm.12919

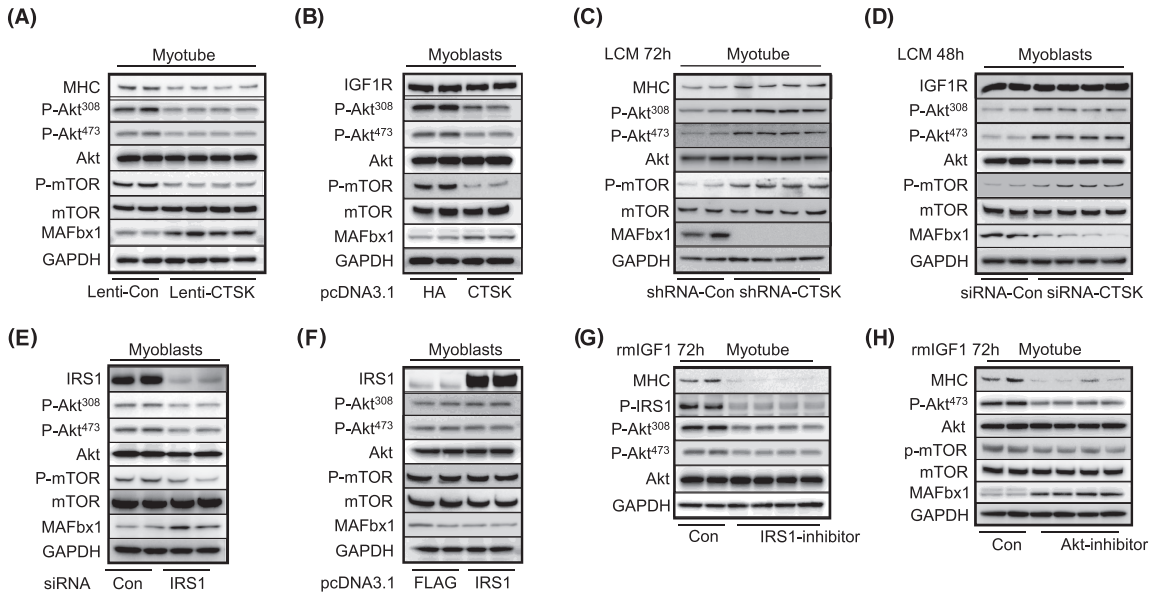

Figure 8 Genetic modifications of CTSK modulate protein catabolism and myosin heavy chain content via regulation of the IRS/Akt 1-signalling pathway. (*A*) C2C12 myoblasts inducible expressing CTSK-HA were grown in differentiation medium for 5 days to differentiate the myoblasts, and then, the cells were treated with DOX for 72 h. Cell lysates were analysed by western blotting using the indicated antibodies. (*B*) C2C12 myoblasts were transiently transfected with pcDNA3.1-HA or pcDNA3.1-CTSK-HA plasmids for 72 h. Cell lysates were analysed by western blotting using the indicated antibodies. (*C*) C2C12 myoblasts stably expressing CTSK-shRNA or Con-shRNA were grown in differentiation medium for 5 days, and then, the cells were cultured with DOX and LCM for 72 h. Cell lysates were analysed by western blotting using the indicated antibodies. (*D*) C2C12 myoblasts were transfected with CTSK-siRNA or Con-siRNA for 24 h, and then, the cells were treated with LCM1/2 for 48 h. Cell lysates were analysed by western blotting using the indicated antibodies. (*E*) C2C12 myoblasts were transfected with IRS-1-siRNA or Con-siRNA for 72 h. Cell lysates were analysed by western blotting using the indicated antibodies. (*F*) C2C12 myoblasts were transiently transfected with pcDNA3.1-3xFLAG or pcDNA3.1-IRS-1-3xFLAG plasmids for 72 h, and then, the cells were lysed in RIPA buffer and analysed by western blotting using the indicated antibodies. (*G*) Following differentiation for 5 days, the cells were treated with hIGF-1 (40 ng/mL) with or without 300 nM of IRS-1 inhibitor (NT157) for 72 h, and then analysed by western blotting using the indicated antibodies. (*H*) Following differentiation for 5 days, the cells were treated with hIGF-1 (40 ng/mL) with/without Akt inhibitor X (2 μM) for 72 h, and finally, the cells were lysed in RIPA buffer and analysed by western blotting using the indicated antibodies.

Discussion

This study focused on molecular close-interactions between CTSK and IRS1 for protein anabolism and catabolism in skeletal muscle cells during the development of cachexia. The significant finding of our present work is that mice lacking the CTSK gene were resistant to cachexia-induced skeletal muscle-mass loss and functional decline following injection with LLC. At the molecular level, CTSK deletion was shown to retard cachectic factor-induced IRS1 degradation and the downstream protein anabolism-related Akt/mTOR signalling inactivation and catabolism-related MAFbx1/MuRF1 activation. In C2C12 cells, silencing or overexpression of CTSK respectively increases or decreases the levels of IRS1 and its downstream anabolic and catabolic signalling, providing the first evidence and mechanistic explanation of CTSK participation in IRS1 signalling in cachectic skeletal muscle wasting and dysfunction (*Figure* S8).

It has been reported that cathepsin is highly expressed in damaged muscles.[16] In this study, we examined changes in CTSK during cancer-induced muscle atrophy and loss of function. From the 14th day after tumour inoculation, CTSK was up-regulated in muscle. The levels of other cathepsins were not significantly changed at this time point. In the present experiment, we demonstrated that TNF-α and LCM regulated the expression of CTSK in skeletal muscle cells. In particular, TNF-α activated the CTSK promoter that induced CTSK expression. And the IGF1/IRS1/Akt pathway has been shown to induce hypertrophy by activating protein synthesis.[12,32] The same pathway can also negatively regulate muscle atrophy markers (MuRF1 and MAFbx1) that induce the degradation of crucial muscle proteins.[33,34] In our model, the IRS1 content was decreased, and imbalanced protein metabolism was displayed on the 28th day after tumour implantation. A previous study concluded that the IGF1/IRS1 pathway is involved in cancer cachexia, but the same also found that IGF1 supplements could not reverse the cancer-induced muscle atrophy in an animal model of cancer cachexia.[35] IRS1 deficiency has been reported to induce muscle atrophy by regulating protein metabolism imbalance *in vivo* and *in vitro*.[36,37] In our present experiments, IRS1 was found to regulate the expression of MAFbx1. We further observed that

silencing of IRS1 increased the levels of MAFbx1 protein in C2C12 cells, whereas overexpression of IRS1 had no effect on the MAFbx1 protein levels. Taken together, these data indicate that IRS1 is required for IGF1/IRS1 signalling-mediated skeletal muscle homeostasis. Consistent with this conclusion, we found that cachexia-induced reduction of IRS1 disturbed the balance of protein metabolism.

It has been reported that calcium/DTT-stimulated IRS1 degradation is inhibited by E-64 (a broad-spectrum inhibitor of cysteine protease).[38] Although the authors' report did not provide direct evidence that cysteine proteases modulate IRS1 degradation, their data suggested this might be the case. In the present study, CTSK enhanced the degradation and ubiquitination level of IRS1. CTSK silencing by the lentivirus rescued LCM-induced IRS1 degradation in the C2C12 myotubes, which further verified our hypothesis. In the IRS1 truncations assay, we found that CTSK did not interact with the $IRS1^{268}$ truncations but bind with the $IRS1^{Fulllength}$, $IRS1^{865}$, and $IRS1^{574}$ truncations. CTSK also selectively promotes the ubiquitination process and degradation of $IRS1^{Fulllength}$, $IRS1^{865}$, and $IRS1^{574}$ truncations, but not $IRS1^{268}$ truncation, indicating that CTSK could mediate the degradation and ubiquitination of IRS1 through its selective impact on the sequence of amino acids 268–574. We found a new IRS1 N-terminal band during co-transfection with CTSK and IRS1 (N-terminal or C-terminal FLAG). These results showed that CTSK-mediated IRS1 degradation represents a common mechanism in modulating skeletal muscle mass and function in mice under cachectic conditions. In addition, a mutation assay showed that CTSK-Y67L and -L205A are necessary for the enzymatic activity of CTSK in IRS1 degradation.

To further confirm that IRS1 degradation induces muscle protein loss, we investigated the effect of IRS1 and Akt phosphorylation on protein metabolism with an IRS1 inhibitor (NT157) or Akt inhibitor (X) in myotubes. Akt has been shown to affect muscle mass by regulating protein catabolism and anabolism.[30,31] In the present study, the IRS1 inhibition decreased the Akt phosphorylation level in C2C12 cells. Pharmacological inhibition of Akt phosphorylation has been shown to promote the expression of MAFbx1, which is associated with protein catabolism.[29,39] Inhibition of Akt phosphorylation also suppresses the phosphorylation of mTOR, which is related to protein synthesis.[13,40] In this study, CTSK silencing by shRNA-CTSK and siRNA-CTSK prevented the degradation of IRS1 and/or the loss of MHC caused by LCM. CTSK silencing also ameliorated the alterations in the levels of $P\text{-}Akt^{308}$, $P\text{-}Akt^{473}$, P-mTOR, and MAFbx1 proteins in C2C12 myotubes and myoblasts in response to LCM1/2, and these beneficial effects were diminished by CTSK overexpression by lentivirus-CTSK or CTSK plasmid. Finally, we verified that the reduction of IRS1 and P-Akt levels contributed to the loss of muscle proteins caused by LCM. IRS1 inhibition decreased the MHC content and also decreased Akt phosphorylation in the myotubes in response to IGF1. Akt inhibition reduced MHC, $P\text{-}Akt^{473}$, and P-mTOR and increased the level of MAFbx1 in the C2C12 myotubes in response to IGF1. Increased CTSK activity appears to promote the loss of skeletal muscle MHC content through its ability to negatively activate anabolic Akt/mTOR signalling and positively activate the catabolic MAFbx1/MuRF1, which was mediated by IRS1 degradation in mice under cachectic conditions.

In the present cachexia model, the histological examination of mice showed that CTSK deficiency effectively reduced cancer-related skeletal muscle mass wasting and dysfunction without affecting tumour growth. Notably, tumour implantation did not change the apoptosis level in skeletal muscle, indicating that muscle atrophy resulted from regulation of the size of individual muscle fibres. This was further confirmed by comparing the sizes of individual muscle sections from WL and KL mice.

Under a cachectic condition, the level of IRS1 in skeletal muscle was higher in KL mice than in WL mice. KL mice showed significantly increased Akt phosphorylation levels, which was consistent with previous studies showing that CTSK deficiency elevated the phosphorylation level of Akt.[21,22] In our experiments, low levels of PI3K, Akt^{308}, Akt^{473}, and mTOR phosphorylation and high levels of the MAFbx1 and MuRF1 proteins were found in WL mice, and the opposite results were observed in KL mice. These data indicate that CTSK ablation reduces the weight loss caused by cancer, and CTSK deficiency causes an activation of the IRS1/Akt pathway and thereby prevents muscle atrophy.

Several limitations should be considered. Mice food intake is not assessed daily. The extensor digitorum longus muscle is not analysed in the present experiments. *Figures* 1C and 2C show the difference of former grip strength changing time might be due to the initial mice body weights, bearing tumour weights, and injected LLCs passages. The mechanism and regulatory factors of CTSK expression under physiological conditions have not been explored.

Conclusions

In summary, our findings have uncovered a new function of cysteinyl CTSK in the regulation of the protein anabolic Akt/mTOR and catabolic MAFbx1/MuRF1 pathways by IRS1 degradation, demonstrating that CTSK deletion partially protects against skeletal muscle atrophy and dysfunction. The results could lead to a novel therapeutic strategy for the control of cancer-induced muscle disease via the regulation of CTSK activity.

Acknowledgements

This work was supported in part by grants from the National Natural Science Foundation of China (Nos. 81770485 and 81560240) and grants from the Ministry of Education, Culture, Sports, Science, and Technology of Japan (Nos. 20H03574, 18K15414, and 20K16518). We thank K. Shimizu and K. Suzuki for their technical assistance. The authors certify that the study complies with the ethical guidelines for publishing in the *Journal of Cachexia, Sarcopenia and Muscle*: update 2017.[41]

Online supplementary material

Additional supporting information may be found online in the Supporting Information section at the end of the article.

Conflicts of interest

The authors declare no conflicts of interest.

References

1. Fearon K, Strasser F, Anker SD, Bosaeus I, Bruera E, Fainsinger RL, et al. Definition and classification of cancer cachexia: an international consensus. *Lancet Oncol* 2011; **12**:489–495.
2. Baracos VE, Martin L, Korc M, Guttridge DC, Fearon KCH. Cancer-associated cachexia. *Nat Rev Dis Primers* 2018;**4**:17105.
3. Mantovani G, Maccio A, Madeddu C, Serpe R, Massa E, Dessi M, et al. Randomized phase III clinical trial of five different arms of treatment in 332 patients with cancer cachexia. *Oncologist* 2010;**15**:200–211.
4. Dunne RF, Mustian KM, Garcia JM, Dale W, Hayward R, Roussel B, et al. Research priorities in cancer cachexia: The University of Rochester Cancer Center NCI Community Oncology Research Program Research Base Symposium on Cancer Cachexia and Sarcopenia. *Curr Opin Support Palliat Care* 2017; **11**:278–286.
5. Prado CMM, Lieffers JR, McCargar LJ, Reiman T, Sawyer MB, Martin L, et al. Prevalence and clinical implications of sarcopenic obesity in patients with solid tumours of the respiratory and gastrointestinal tracts: a population-based study. *Lancet Oncol* 2008;**9**:629–635.
6. von Haehling S, Anker SD. Prevalence, incidence and clinical impact of cachexia: facts and numbers-update 2014. *J Cachexia Sarcopenia Muscle* 2014;**5**:261–263.
7. Cohen S, Nathan JA, Goldberg AL. Muscle wasting in disease: molecular mechanisms and promising therapies. *Nat Rev Drug Discov* 2015;**14**:58–74.
8. Fearon K, Arends J, Baracos V. Understanding the mechanisms and treatment options in cancer cachexia. *Nat Rev Clin Oncol* 2012;**10**:90–99.
9. Costelli P, Carbo N, Tessitore L, Bagby GJ, Lopez-Soriano FJ, Argiles JM, et al. Tumor necrosis factor-alpha mediates changes in tissue protein turnover in a rat cancer cachexia model. *J Clin Invest* 1993;**92**: 2783–2789.
10. Han J, Meng Q, Shen L, Wu G. Interleukin-6 induces fat loss in cancer cachexia by promoting white adipose tissue lipolysis and browning. *Lipids Health Dis* 2018;**17**:14.
11. Brown JL, Lee DE, Rosa-Caldwell ME, Brown LA, Perry RA, Haynie WS, et al. Protein imbalance in the development of skeletal muscle wasting in tumour-bearing mice. *J Cachexia Sarcopenia Muscle* 2018; **9**:987–1002.
12. Sacheck JM, Ohtsuka A, McLary SC, Goldberg AL. IGF-I stimulates muscle growth by suppressing protein breakdown and expression of atrophy-related ubiquitin ligases, atrogin-1 and MuRF1. *Am J Physiol Endocrinol Metab* 2004;**287**:E591–E601.
13. Saxton RA, Sabatini DM. mTOR signaling in growth, metabolism, and disease. *Cell* 2017;**168**:960–976.
14. Tanaka M, Sugimoto K, Fujimoto T, Xie K, Takahashi T, Akasaka H, et al. Differential effects of pre-exercise on cancer cachexia-induced muscle atrophy in fast- and slow-twitch muscles. *FASEB J* 2020;**34**: 14389–14406.
15. Yoshikawa T, Noguchi Y, Satoh S. Inhibition of IRS-1 phosphorylation and the alterations of GLUT4 in isolated adipocytes from cachectic tumor-bearing rats. *Biochem Biophys Res Commun* 1999;**256**: 676–681.
16. Ogasawara S, Cheng XW, Inoue A, Hu L, Piao L, Yu C, et al. Cathepsin K activity controls cardiotoxin-induced skeletal muscle repair in mice. *J Cachexia Sarcopenia Muscle* 2018;**9**:160–175.
17. Hummel RP 3rd, James JH, Warner BW, Hasselgren PO, Fischer JE. Evidence that cathepsin B contributes to skeletal muscle protein breakdown during sepsis. *Arch Surg* 1988;**123**:221–224.
18. Verbovsek U, Van Noorden CJ, Lah TT. Complexity of cancer protease biology: cathepsin K expression and function in cancer progression. *Semin Cancer Biol* 2015;**35**: 71–84.
19. Brubaker KD, Vessella RL, True LD, Thomas R, Corey E. Cathepsin K mRNA and protein expression in prostate cancer progression. *J Bone Miner Res* 2003;**18**:222–230.
20. Dauth S, Arampatzidou M, Rehders M, Yu DMT, Führer D, Brix K. Thyroid cathepsin K: roles in physiology and thyroid disease. *Clin Rev Bone Mineral Metab* 2011;**9**: 94–106.
21. Guo R, Hua Y, Ren J, Bornfeldt KE, Nair S. Cardiomyocyte-specific disruption of cathepsin K protects against doxorubicin-induced cardiotoxicity. *Cell Death Dis* 2018;**9**:692.
22. Guo R, Hua Y, Rogers O, Brown TE, Ren J, Nair S. Cathepsin K knockout protects against cardiac dysfunction in diabetic mice. *Sci Rep* 2017;**7**:8703.
23. Hua Y, Zhang Y, Dolence J, Shi GP, Ren J, Nair S. Cathepsin K knockout mitigates high-fat diet-induced cardiac hypertrophy and contractile dysfunction. *Diabetes* 2013;**62**:498–509.
24. Yang M, Sun J, Zhang T, Liu J, Zhang J, Shi MA, et al. Deficiency and inhibition of cathepsin K reduce body weight gain and increase glucose metabolism in mice. *Arterioscler Thromb Vasc Biol* 2008;**28**: 2202–2208.
25. Wang X, Lin Y. Tumor necrosis factor and cancer, buddies or foes? *Acta Pharmacol Sin* 2008;**29**:1275–1288.
26. Lecaille F, Choe Y, Brandt W, Li Z, Craik CS, Bromme D. Selective inhibition of the collagenolytic activity of human cathepsin K by altering its S2 subsite specificity. *Biochemistry* 2002;**41**:8447–8454.
27. Kim S, Jin H, Seo HR, Lee HJ, Lee YS. Regulating BRCA1 protein stability by cathepsin S-mediated ubiquitin degradation. *Cell Death Differ* 2019;**26**:812–825.
28. Zhang C, Zhang M, Song S. Cathepsin D enhances breast cancer invasion and metastasis through promoting hepsin ubiquitin-proteasome degradation. *Cancer Lett* 2018;**438**:105–115.

29. Zhang G, Jin B, Li YP. C/EBPbeta mediates tumour-induced ubiquitin ligase atrogin1/MAFbx upregulation and muscle wasting. *EMBO J* 2011;**30**:4323–4335.
30. Schmitt TL, Martignoni ME, Bachmann J, Fechtner K, Friess H, Kinscherf R, et al. Activity of the Akt-dependent anabolic and catabolic pathways in muscle and liver samples in cancer-related cachexia. *J Mol Med (Berl)* 2007;**85**:647–654.
31. Bodine SC, Stitt TN, Gonzalez M, Kline WO, Stover GL, Bauerlein R, et al. Akt/mTOR pathway is a crucial regulator of skeletal muscle hypertrophy and can prevent muscle atrophy in vivo. *Nat Cell Biol* 2001;**3**:1014–1019.
32. Yoshida T, Delafontaine P. Mechanisms of IGF-1-mediated regulation of skeletal muscle hypertrophy and atrophy. *Cell* 2020;**9**:1970.
33. Nakao R, Hirasaka K, Goto J, Ishidoh K, Yamada C, Ohno A, et al. Ubiquitin ligase Cbl-b is a negative regulator for insulin-like growth factor 1 signaling during muscle atrophy caused by unloading. *Mol Cell Biol* 2009;**29**:4798–4811.
34. Shi J, Luo L, Eash J, Ibebunjo C, Glass DJ. The SCF-Fbxo40 complex induces IRS1 ubiquitination in skeletal muscle, limiting IGF1 signaling. *Dev Cell* 2011;**21**:835–847.
35. Penna F, Bonetto A, Muscaritoli M, Costamagna D, Minero VG, Bonelli G, et al. Muscle atrophy in experimental cancer cachexia: is the IGF-1 signaling pathway involved? *Int J Cancer* 2010;**127**:1706–1717.
36. Araki E, Lipes MA, Patti ME, Bruning JC, Haag B 3rd, Johnson RS, et al. Alternative pathway of insulin signalling in mice with targeted disruption of the IRS-1 gene. *Nature* 1994;**372**:186–190.
37. Tamemoto H, Kadowaki T, Tobe K, Yagi T, Sakura H, Hayakawa T, et al. Insulin resistance and growth retardation in mice lacking insulin receptor substrate-1. *Nature* 1994;**372**:182–186.
38. Smith LK, Rice KM, Garner CW. The insulin-induced down-regulation of IRS-1 in 3T3-L1 adipocytes is mediated by a calcium-dependent thiol protease. *Mol Cell Endocrinol* 1996;**122**:81–92.
39. Gomes MD, Lecker SH, Jagoe RT, Navon A, Goldberg AL. Atrogin-1, a muscle-specific F-box protein highly expressed during muscle atrophy. *Proc Natl Acad Sci U S A* 2001;**98**:14440–14445.
40. Risson V, Mazelin L, Roceri M, Sanchez H, Moncollin V, Corneloup C, et al. Muscle inactivation of mTOR causes metabolic and dystrophin defects leading to severe myopathy. *J Cell Biol* 2009;**187**:859–874.
41. von Haehling S, Morley JE, Coats AJS, Anker SD. Ethical guidelines for publishing in the Journal of Cachexia Sarcopenia and Muscle: update 2019. *J Cachexia Sarcopenia Muscle* 2019;**10**:1143–1145.